

A Robust Pixel ECC based Algorithm for Occluded Image Alignment

Nefeli Lamprinou and Emmanouil Z. Psarakis

Department of Computer Engineering and Informatics, University of Patras, 26504 Rio-Patras, Greece

Keywords: Image Alignment, Occluded Images, Correlation Coefficient.

Abstract: The alignment of occluded images constitutes a common and difficult problem. In this paper we propose a new method based on ECC algorithm tailored to occluded image alignment problem which enjoy a simple closed-form solution with low computational cost. Moreover, the use of a proper subset of the region of interest that limits the impact of the outliers in the estimation of the parameters is proposed. The use of this set seems to make the proposed method insensitive to the use of the occluded image as template or as warped in the alignment process. The proposed method is compared against two well known Gradient Correlation based methods by its application in several image alignment problems and in all cases outperforms its rivals in terms of accuracy and percentage of convergence.

1 INTRODUCTION

Image registration methods aim at finding the corresponding points in two or more images and align them by moving their data to a common coordinate system. So alignment means to restore the geometric deformations that exist between the images. Solving the alignment problem is essential to many different high level applications such as face or object recognition, motion analysis and medical imaging. A demanding problem is face alignment, especially in cases where real images are considered, due to many different conditions during image capture such as face expressions, lighting conditions and occlusions (sunglasses, scarf etc.).

Alignment methods aim to estimate the parameters of the geometric transformation between a template and an observation image, which can be achieved through the optimization of a cost or similarity function. Referring to area based techniques LK algorithm (Lucas and Kanade, 1981) is the most popular method based on the minimization of the l_2 norm of the error between the images. The original LK algorithm, however, is inefficient in the presence of outliers, which constitutes a very common problem when using real images with uncontrolled lighting conditions and occlusions. So numerous variations and extensions of the LK algorithm have been proposed through the years to address this problem such as FM (Fuh and Maragos, 1991), weighted LK (Baker and Matthews, 2004), Fourier LK (S. Lucey and Sridha-

ran, 2012) and (A.B. Ashraf and Chen, 2010).

A different approach in solving the alignment problem is the maximization of a similarity function with the most known one being the correlation coefficient. Existing similarities and differences of the above mentioned approach with l_2 based one can be found in (Evangelidis and Psarakis, 2008) where the ECC, an algorithm that uses the above similarity measure on image intensities, was introduced. Similarly, Gradient Correlation algorithm (G. Tzimiropoulos and Pantic, 2011) maximizes the correlation of image gradient orientations (G. Tzimiropoulos, 2010), an approach that is able to address the problem of non uniform photometric distortions and occlusions, although the use of face features reduces its performance in images with different content.

In this paper we focus on the alignment of occluded images, that constitutes a common and difficult problem (F. Yang and Metaxas, 2011), (G. Yang and Lu, 2015), and the use of an ECC based algorithm, applied in each pixel is proposed. Specifically, we propose the maximization of the correlation between the image gradients at every pair of corresponding pixels separately, leading to a global estimation of the distortion parameters. Since in the problem we address, there is a large number of outliers, not all pixels must be used during the optimization. To this end we propose a criterion that excludes a large number or even all of the pixels within the occluded regions, ensuring that the outliers have a minimum contribution in the final estimation. In addition, the proposed

closed form solution results in a computational efficient, as well as robust, algorithm.

The paper is organized as follows. In Section 2 the problem formulation is presented and the pixel-ECC approach is introduced. In Section 3 the image alignment problem is formulated and the proposed optimization problem is solved. In Section 4 the results we obtained from the application of the proposed algorithm in the experiments we have conducted, are presented. Finally, Section 5 contains our conclusions and future directions.

2 PROBLEM FORMULATION

Let us consider that the photometric distortions are local and they can be modeled as follows;

$$g(\mathbf{x}_i) = \alpha_i f(\mathbf{x}_i) + \beta_i, \quad i = 1, 2, \dots, N \quad (1)$$

where $f(\cdot)$, $g(\cdot)$ denote the intensities of the \mathbf{x}_i -th pixel of the template and the warped and photometrically distorted image respectively, and N is the total number image's pixel.

As it is clear from (1), the photometric distortion is modeled by the use of the multiplicative and the additive parameter α_i and β_i respectively. Actually, we can easily remove the effects of the additive parameter by evaluating the gradient of the intensity function at each one pixel. Moreover, in order to remove the effects of the multiplicative parameter we are going to use the cost function introduced in (Evangelidis and Psarakis, 2008), but by defining it using a pair of corresponding pixels. To this end let us define the following quantity:

$$\mathbf{t}_i = \nabla f(\mathbf{x}_i) = \left[\frac{\partial f(\mathbf{x}_i)}{\partial x_{i1}} \quad \frac{\partial f(\mathbf{x}_i)}{\partial x_{i2}} \right]^T$$

and its normalized counterpart:

$$\bar{\mathbf{t}}_i = \frac{\nabla f(\mathbf{x}_i)}{\|\nabla f(\mathbf{x}_i)\|_2} \quad (2)$$

where $\|\mathbf{x}\|_2$ denotes the l_2 norm of vector \mathbf{x} .

Then, for the i -th pair of the corresponding pixels we define the following cost function:

$$\varepsilon_i(\mathbf{p}) = \|\bar{\mathbf{t}}_i - \bar{\mathbf{q}}_i(\mathbf{p})\|_2^2 \quad (3)$$

and we would like to minimize it w.r.t. the vector geometric distortion parameters \mathbf{p} . The above defined minimization problem, as it was proved in (Evangelidis and Psarakis, 2008), is equivalent with the maximization of the following quantity which is known in the literature as Enhanced Correlation Coefficient (ECC):

$$\rho(\mathbf{p}) = \langle \bar{\mathbf{t}}_i, \bar{\mathbf{q}}_i(\mathbf{p}) \rangle \quad (4)$$

where $\langle \mathbf{x}, \mathbf{y} \rangle$ denotes the inner product of the vectors \mathbf{x} , \mathbf{y} . Since, the similarity function defined by (4) is a nonlinear function of the parameter vector \mathbf{p} , we are going to linearize it and thus replacing the original optimization problem with a sequence of secondary ones. To this end we adopt the forward additive updating rule expressed by the following equation:

$$\mathbf{p}_n \leftarrow \mathbf{p}_{n-1} + \Delta \mathbf{p}_n \quad (5)$$

and use the Taylor expansion of the warped image, i.e.:

$$\begin{aligned} \mathbf{q}_i(\mathbf{p}_n) &= \mathbf{q}_i(\mathbf{p}_{n-1} + \Delta \mathbf{p}_n) \\ &= \mathbf{q}_i(\mathbf{p}_{n-1}) + H_i(I_2 \otimes \bar{\mathbf{x}}_i') \Delta \mathbf{p}_n \end{aligned} \quad (6)$$

where H_i is the 2×2 Hessian matrix of warped intensity function on the i -th pixel having homogeneous coordinates $\bar{\mathbf{x}}_i$, I_2 the 2×2 eye matrix and \otimes is denoting the kronecker product operator. For simplicity reasons we drop the dependency of the warped vectors on the parameter vector \mathbf{p} and the dependency of the updating rule on n .

By setting:

$$\mathbf{z}_i = H_i(I_2 \otimes \bar{\mathbf{x}}_i') \Delta \mathbf{p} \quad (7)$$

and substituting it into (6), Equation (4) can be expressed as follows:

$$\rho(\mathbf{z}_i) = \frac{\bar{\mathbf{t}}_i^T \mathbf{q}_i + \bar{\mathbf{t}}_i^T \mathbf{z}_i}{\sqrt{\|\mathbf{q}_i\|_2^2 + 2\mathbf{q}_i^T \mathbf{z}_i + \|\mathbf{z}_i\|_2^2}} \quad (8)$$

and our goal is to maximize it w.r.t. \mathbf{z}_i . This is achieved by the next *lemma*.

Lemma 1. Let us consider that we would like to maximize the similarity function defined by (8) w.r.t. the vector \mathbf{z}_i . Assuming the invertibility of matrix H_i , the similarity function attains its maximum value, i.e. $\rho(\mathbf{z}_i) = 1$, iff vector \mathbf{z}_i^* is of the following form:

$$\mathbf{z}_i^* = \lambda_i \bar{\mathbf{t}}_i - \mathbf{q}_i \quad (9)$$

where λ_i is a positive number.

Proof: The proof of the lemma is simple and is omitted. \square

As it is clear from *Lemma 1*, the parameter λ_i models the photometric distortion related to the i -th pixel of the photometrically distorted image. We must stress at this point that the only constraint that must be imposed, is the positivity of the parameter λ_i .

Concluding, we would like to remove the local photometric distortions existing in corresponding pixels by using their gradients denoted by the vectors $\bar{\mathbf{t}}_i$ and $\bar{\mathbf{q}}_i$ respectively and the vector \mathbf{z}_i defined by (7). This is exactly our goal in the next section.

3 THE ALIGNMENT PROBLEM

Let us now reformulate the image matching problem by taking into account all the quantities defined in the previous section. To this end let us consider that for each member of the following pixel subset of the region of interest \mathcal{R} :

$$\mathcal{P} = \{\mathbf{x}_k \in \mathcal{R}, k = 1, \dots, K\} \quad (10)$$

there is $\lambda_k > 0$ such that equation (9) can be satisfied (i.e. pixels \mathbf{x}_k and $\mathbf{W}(\mathbf{x}_k; \mathbf{p})$, associated with the template and the warped intensities $f(\mathbf{x}_k)$ and $g(\mathbf{W}(\mathbf{x}_k; \mathbf{p}))$ respectively, constitute a pair of corresponding pixels, where $\mathbf{W}(\mathbf{x}; \mathbf{p})$ denotes a geometric transformation parametrized by vector \mathbf{p}). Then, using Lemma 1 in each pair of corresponding pixels contained in the above defined set and by taking into account that in the general case $K \gg 6$, we obtain the following overdetermined linear system of equations:

$$(I_2 \otimes \tilde{\mathbf{x}}_k^t) \Delta \mathbf{p} = H_k^{-1} (\lambda_k \bar{\mathbf{t}}_k - \mathbf{q}_k), k = 1, 2, \dots, K \quad (11)$$

whose the solution we are going to investigate in the next paragraph.

3.1 An l_2 based Solution

As it was already mentioned, the linear system of equations defined by (11) is overdetermined and thus, in the general case, it has not an exact solution. In order to overcome this obstacle we are going to find an approximate solution which will be optimum in the l_2 sense.

To this end let us define the following quantities:

$$\begin{aligned} X &= \{I_2 \otimes \tilde{\mathbf{x}}_k^t\}_{k=1}^K \\ D &= -\text{diag}\{H_k^{-1} \bar{\mathbf{t}}_k\}_{k=1}^K \\ \mathbf{b} &= -\{H_k^{-1} \mathbf{q}_k\}_{k=1}^K \\ \lambda &= \{\lambda_k\}_{k=1}^K \end{aligned} \quad (12)$$

where X is a $2K \times 6$ matrix, D is a $2K \times K$ block diagonal matrix and \mathbf{b} , λ column vectors of length $2K$ and K respectively.

Then, the linear system defined by (11) can be rewritten as follows:

$$\begin{pmatrix} X & D \end{pmatrix} \begin{pmatrix} \Delta \mathbf{p} \\ \lambda \end{pmatrix} = \mathbf{b}. \quad (13)$$

and we would like to solve the following optimization problem:

$$\min_{\Delta \mathbf{p}, \lambda} \left\| \begin{pmatrix} X & D \end{pmatrix} \begin{pmatrix} \Delta \mathbf{p} \\ \lambda \end{pmatrix} - \mathbf{b} \right\|_2^2 \quad (14)$$

whose the optimal solution can be easily proved that is given by the following relation:

$$\begin{pmatrix} \Delta \mathbf{p}^* \\ \lambda^* \end{pmatrix} = \begin{pmatrix} X^T X & X^T D \\ D^T X & D^T D \end{pmatrix}^{-1} \begin{pmatrix} X^T \\ D^T \end{pmatrix} \mathbf{b}. \quad (15)$$

To avoid numerical problems and reduce the computational cost, we exploit the special form of the above linear system and propose to use instead the following equations:

$$X^T X \Delta \mathbf{p} + X^T D \lambda = X^T \mathbf{b} \quad (16)$$

$$D^T X \Delta \mathbf{p} + D^T D \lambda = D^T \mathbf{b}. \quad (17)$$

Solving (17) for λ and substituting into (16) we obtain:

$$\Delta \mathbf{p}^* = (X^T (I_{2K} - \mathbb{P}_D) X)^{-1} X^T (I_{2K} - \mathbb{P}_D) \mathbf{b} \quad (18)$$

where matrix \mathbb{P}_D is the following projection matrix:

$$\mathbb{P}_D = D(D^T D)^{-1} D^T.$$

Note that the matrix $D^T D$ is diagonal and consequently its inverse is easily computed.

3.2 Defining Subset \mathcal{P}

In order to complete the proposed technique, we have yet to define the pixel subset of (10). To achieve our goal we are going to exploit the special form of the linear system (17). To this end we use the quantities defined in (12), and re-express it as follows:

$$-\bar{\mathbf{t}}_k^t H_k^{-1} (I_2 \otimes \tilde{\mathbf{x}}_k^t) \Delta \mathbf{p} + \|H_k^{-1} \bar{\mathbf{t}}_k\|_2^2 \lambda_k = \bar{\mathbf{t}}_k^t H_k^{-2} \mathbf{q}_k \quad (19)$$

where $k = 1, 2, \dots, K$.

As we can see, when we are close to the optimum warp (i.e. $\Delta \mathbf{p} \rightarrow \mathbf{0}_6$) each one of the above mentioned equation can be written as follows:

$$\bar{\mathbf{t}}_k^t H_k^{-1} (H_k^{-1} \bar{\mathbf{t}}_k \lambda_k - H_k^{-1} \mathbf{q}_k) \approx \mathbf{0}_2. \quad (20)$$

Since $H_k^{-1} \bar{\mathbf{t}}_k$, in the general case is not equal to zero, we have that the vector $H_k^{-1} \bar{\mathbf{t}}_k \lambda_k - H_k^{-1} \mathbf{q}_k$ must be close to $\mathbf{0}_2$. Note that in the ideal case

$$H_k^{-1} \bar{\mathbf{t}}_k \lambda_k = H_k^{-1} \mathbf{q}_k$$

and the above equations have a unique solution for the parameter λ_k , that is $\lambda_k = \|\mathbf{q}_k\|_2$ and this in turn ensures the desired positivity of λ . However, when we are not close to the optimal solution the above mentioned equality does not hold for any pair of corresponding pixels and as an alternative we propose to define the pixel subset \mathcal{P} as follows:

$$\mathcal{P} = \cap_{i=1}^3 \mathcal{R}_i, \quad (21)$$

where:

$$\begin{aligned} \mathcal{R}_1 &= \{\tilde{\mathbf{x}}_k \in \mathcal{R} : \text{sign}(H_k^{-1} \bar{\mathbf{t}}_k) = \text{sign}(H_k^{-1} \mathbf{q}_k)\} \\ \mathcal{R}_2 &= \{\tilde{\mathbf{x}}_k \in \mathcal{R} : \text{sign}(H_{f_k}^{-1} \bar{\mathbf{t}}_k) = \text{sign}(H_{f_k}^{-1} \mathbf{q}_k)\} \\ \mathcal{R}_3 &= \{\tilde{\mathbf{x}}_k \in \mathcal{R} : \text{sign}(H_k^{-1} \bar{\mathbf{t}}_k) = \text{sign}(H_{f_k}^{-1} \bar{\mathbf{t}}_k)\} \end{aligned}$$

and H_{f_k} denotes the 2×2 Hessian matrix of the template intensity function on the k -th pixel with coordinates \mathbf{x}_k . Note that through the use of sets \mathcal{R}_2 and \mathcal{R}_3 we impose, in some sense, the desired insensitivity of the proposed algorithm independently if we use the occluded image in the alignment process as the template or as the warped one.

It is clear that the above defined set \mathcal{P} changes in each iteration of the algorithm. In Figure 1 instances of the evolution of the set \mathcal{P} for four different examples are shown. From this figure it is clear that the cardinality of these sets is an increasing sequence of the iteration number. Note also the impact of the proposed constraints in the formation of the set. Pixels that belong into occluded regions, with high probability, are not members of the aforementioned sets. This is apparent in the last three rows of Figure 1 where the proposed technique is applied for the alignment of occluded images.

The outline of the proposed algorithm follows.

Algorithm 1: Pixel Based ECC Image Alignment Algorithm. Input: Template $f(\cdot)$ and Warped $g(\cdot)$ Images.

- 1: Compute the gradient of the template image $f(\cdot)$ and its hessian.
- 2: **repeat**
- 3: Compute the gradient of the warped image $g(\cdot)$ and its hessian.
- 4: Using (21) define the pixel subset \mathcal{P} .
- 5: Using (18) compute $\Delta \mathbf{p}^*$.
- 6: Use (5) to update the parameter vector \mathbf{p} .
- 7: Update the warped image
- 8: **until** convergence
- 9: Output: The warp.

Having completed the presentation of the proposed technique, we are going to apply it in the next section.

4 EXPERIMENTS

In this section we are going to apply the proposed alignment technique by conducting a couple of experiments. In addition we will compare its performance in terms of the achieved alignment error, as well as its frequency of convergence against the methods proposed in (G. Tzimiropoulos and Pantic, 2011); namely GradientImages and Gradient-Corr. We assessed the performance of rivals by using the performance evaluation framework proposed in (Baker and Matthews, 2004) that has been adopted by other researchers (Evangelidis and Psarakis, 2008), (A.B. Ashraf and Chen, 2010) as a standard for that

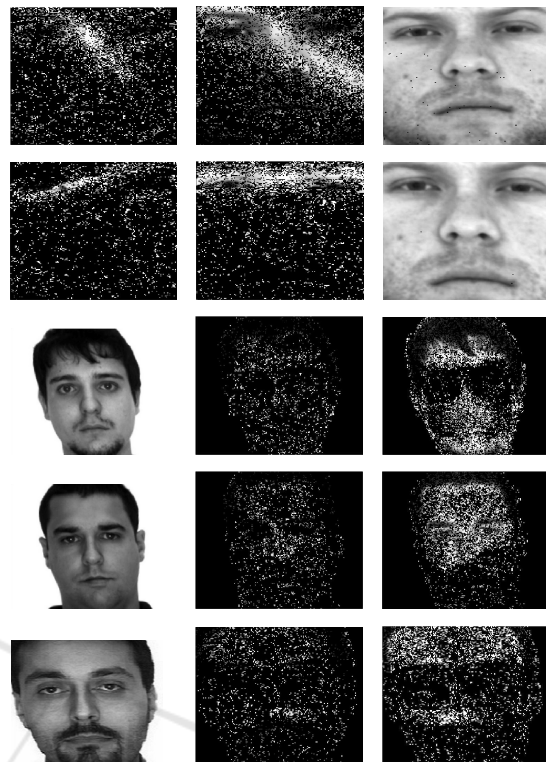


Figure 1: Pixel subset \mathcal{P} defined in (21). *First line:* Subset \mathcal{P} for a nonoccluded image with $\sigma = 5$ in the 1-st, 5-th and 10-th iteration. *Second line:* Subset \mathcal{P} for the same image but with $\sigma = 15$ in the 1-st, 40-th and 60-th iteration. *Third line:* The template image with $\sigma = 10$ aligned with sunglasses occluded image and the pixel subset \mathcal{P} in the 1-st and 30-th iteration. *Fourth line:* The template image with $\sigma = 10$ aligned with scarf occluded image and the pixel subset \mathcal{P} in the 1-st and 30-th iteration. *Fifth line:* The template image with $\sigma = 10$ aligned with mixed sunglasses and scarf occluded image and the pixel subset \mathcal{P} in the 1-st and 30-th iteration.

purpose. This framework is briefly summarized in the next paragraph.

4.1 Experimental Setup

The evaluation in (Baker and Matthews, 2004) is as follows. We select a Region of Interest (RoI) (please see Figure 2) and three canonical points in this region. We perturb these points using Gaussian noise of standard deviation σ and compute the initial RMS Distance (RMSD) between the canonical and perturbed points. Using the affine warp that the original and perturbed points define, we generate the affine distorted image. Given a warp estimate, we compute the destination of the three canonical points and, then, the final RMSD between the estimated and correct locations. We use RMSD for a fixed Point Standard Deviation σ and the Percentage of Converging (POC) runs for sev-

eral values of σ as figures of merit for the performance evaluation. An algorithm is considered as converged if the final RMSD was less than 3 pixels after 60 iterations in total. In particular, for the efficient implementation of the proposed algorithm we have used a three level pyramid dividing the above mentioned iterations into 30, 20 and 10 in each level of the pyramid respectively. In all experiments we used the Matlab code provided by the authors of (G. Tzimiropoulos and Pantic, 2011).

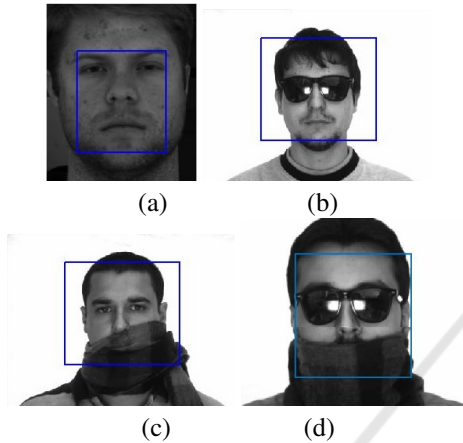


Figure 2: Different forms of Regions of interest (RoI) which are used in our experiments (please see the text for the details).

4.2 Experiment I

In this experiment we are going to apply the rivals on geometrically distorted images without photometric distortions or occlusions by using the RoI shown in Figure 2.a. For all the results we obtained we used, for each σ , 30 randomly generated warps in ten different images from Yale B database (A.S. Georghiadis and Kriegman, 2001). The resulting Percentage of Converging runs of the rivals with the size of the geometric distortion $\sigma \in [5, 15]$ from their application on face images from the Yale B database are shown in Figure 3. As we can see the proposed technique outperforms its rivals.

In addition, Table 1 contains the RMS Distances achieved by the rivals, in converging runs, with the σ taking the above mentioned values. As it is clear from this table, the proposed technique achieves the smallest RMSD even in the strongest geometric distortions.

4.3 Experiment II

In addition to the standard Yale B based Experiment I, we considered the problem of face alignment in the presence of real strong occlusions by using face images from the AR database (Martinez and Benavente,

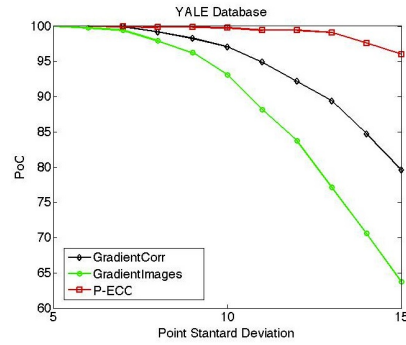


Figure 3: Frequency of Convergence versus Point Standard Deviation $\sigma \in [5, 15]$ for images from Yale B database.

Table 1: RMS Distances obtained from the application of the rivals on images from Yale B database.

σ	GradientIm	GradientCorr	P-ECC
5	6.0×10^{-02}	3.0×10^{-02}	1.9×10^{-10}
6	7.0×10^{-02}	5.0×10^{-02}	1.9×10^{-10}
7	1.0×10^{-01}	6.0×10^{-02}	1.7×10^{-09}
8	1.1×10^{-01}	6.0×10^{-02}	2.3×10^{-09}
9	1.5×10^{-01}	1.1×10^{-01}	3.0×10^{-07}
10	1.7×10^{-01}	1.3×10^{-01}	1.0×10^{-04}
11	2.1×10^{-01}	1.3×10^{-01}	6.3×10^{-03}
12	7.1×10^{-01}	6.8×10^{-01}	6.4×10^{-03}
13	8.8×10^{-01}	7.8×10^{-01}	6.4×10^{-03}
14	1.02	8.8×10^{-01}	5.1×10^{-02}
15	1.21	9.1×10^{-01}	5.8×10^{-02}

1998). More specifically, we applied the rivals on the sunglasses and scarf occluded images contained in the AR database and on mixed sunglasses and scarf images we created. The Regions of Interest we have used for the above mentioned categories are shown in Figures 2.(b), 2.(c) and 2.(d) respectively. Note that in this database the sunglasses and scarf images are already geometrically distorted w.r.t. the template ones, occasionally including large rotation and/or translation distortions. In order to be able to correctly measure RMSD we estimated the original transform and then subtracted it from the final estimations. Thus, in this experiment we have used only the images where we were able to achieve a high quality original alignment. This is also the reason why the RoI we have used in this case is larger than the corresponding one in Yale B (see Figure 2).

For the results we obtained for the sunglasses images we used, for each σ , 25 randomly generated warps in 24 different images, for the scarf images we used, for each σ , 20 randomly generated warps in 26 different images while for the mixed sunglasses and scarf images we used, for each σ , 30 randomly generated warps in 12 different images.

The resulting Percentage of Converging runs of

the rivals with the size of the geometric distortion $\sigma \in [1, 10]$ are shown in Figures 4, 5 and 6 respectively. As we can see from these figures the proposed technique outperforms again its rivals.

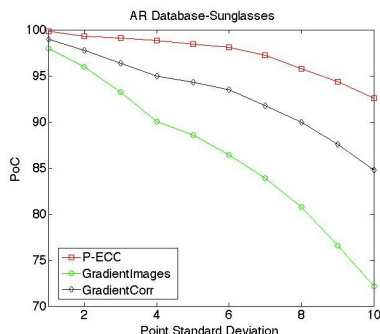


Figure 4: Frequency of Convergence versus Point Standard Deviation $\sigma \in [1, 10]$ for Sunglasses images from AR database.



Figure 5: Frequency of Convergence versus Point Standard Deviation $\sigma \in [1, 10]$ for Scarf images from AR Database.

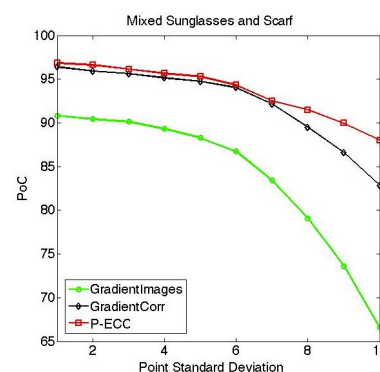


Figure 6: Frequency of Convergence versus Point Standard Deviation $\sigma \in [1, 10]$ for the mixed Sunglasses and Scarf images from AR database.

5 CONCLUSIONS

In this paper a new occluded image alignment method based on ECC algorithm was proposed. The optimal parameters were obtained by iteratively solving a sequence of approximate nonlinear optimization problems which enjoy a simple closed-form solution with low computational cost. The proposed method was compared against two well known Gradient Correlation methods through two experiments. In all cases, the proposed algorithm was outperforming its rivals in terms of accuracy and percentage of convergence. The extension of the proposed algorithm for the problem of image alignment under strong photometric distortions is under investigation.

REFERENCES

- A.B. Ashraf, S. L. and Chen, T. (2010). Fast image alignment in the fourier domain. *Proceedings of CVPR*, pages 2480–2487.
- A.S. Georghiades, P. B. and Kriegman, D. (2001). *From few to many: Illumination cone models for face recognition under variable lighting and pose*.
- Baker, S. and Matthews, I. (2004). Lucas-kanade 20 years on: A unifying framework. *International Journal in Computer Vision*, 56, no. 3:221–255.
- Evangelidis, G. and Psarakis, E. (2008). Parametric image alignment using enhanced correlation coefficient maximization. *IEEE Transactions on Pattern Analysis and Machine Intelligence*, pages 1858–1865.
- F. Yang, J. H. and Metaxas, D. (2011). Sparse shape registration for occluded facial feature localization. *IEEE Conference on Automatic Face and Gesture Recognition*.
- Fuh, C. and Maragos, P. (1991). Motion displacement estimation using an affine model for image matching. *Optical Eng.*, 30, no. 7:881–887.
- G. Tzimiropoulos, S. Z. and Pantic, M. (2011). Robust and efficient parametric face alignment. *IEEE International Conference on Computer Vision (ICCV)*.
- G. Yang, Y. F. and Lu, H. (2015). Sparse error via reweighted low rank representation for face recognition with various illumination and occlusion. *International Journal for light and electron optics*.
- G.Tzimiropoulos, V.Argyriou, S. a. T. (2010). Robust fft-based scale-invariant image registration with image gradients. *IEEE Transactions on Pattern Analysis and Machine Intelligence*, pages 1899–1906.
- Lucas, B. and Kanade, T. (1981). An iterative image registration technique with an application to stereo vision. *Proc. Seventh Intl Joint Conf. Artificial Intelligence*.
- Martinez, A. and Benavente, R. (1998). *The Book*. CVC Technical Report 24.
- S. Lucey, R. Navarathna, A. B. A. and Sridharan, S. (2012). Fourier lucas-kanade algorithm. *IEEE Transactions on Pattern Analysis and Machine Intelligence*, 6, no. 1.